A WAY TO ASSESS THE IMPAIRMENT OF CEREBRAL AUTOREGULATION IN PEDIATRIC PATIENTS UNDER ECMO WITH NEUROIMAGING ABNORMALITIES

by

SYLVINE INEZA

Presented to the Faculty of the Honors College of

The University of Texas at Arlington in Partial Fulfillment

of the Requirements

for the Degree of

HONORS BACHELOR OF SCIENCE IN BIOMEDICAL ENGINEERING

THE UNIVERSITY OF TEXAS AT ARLINGTON

May 2023

ACKNOWLEDGMENTS

I am grateful to God, my mentors and my friends who have supported me through this brilliant journey at The University of Texas at Arlington. They have helped me time and again. My path has not been without challenges, but all the fights have been worth it. Every obstacle has made me better and improved my approach to life. And sometimes I have failed too but learning from those downturns and coming back stronger is what allowed me to progress quickly despite setbacks.

I also want to specially thank Dr. Liu for believing in me and giving me the opportunity to work as an undergraduate research assistant in her lab even with my limited experience. In the lab, I had an amazing lab partner, Sheetala, who trained me and was of tremendous support; always ready to help and encouraged me to keep pushing. She was a friend and a guide.

To my parents, my rock, thanks for having my back through it all. Even the smallest of sacrifices never went unnoticed! They invested in me and inspired me to keep dreaming and pushing. I could not have done it without them. Last but not least, I would like to extend my gratitude and appreciation to the BE department in the College of Engineering that aided my ventures through various opportunities and sponsorships, not forgetting the Honors College through which this publication is made possible.

May 12, 2023

ABSTRACT

A WAY TO ASSESS THE IMPAIRMENT OF CEREBRAL AUTOREGULATION IN PEDIATRIC PATIENTS UNDER ECMO WITH NEUROIMAGING ABNORMALITIES

Sylvine Ineza, B.S. Biomedical Engineering

The University of Texas at Arlington, 2023

Faculty Mentor: Hanli Liu

Cerebral autoregulation protects the healthy brain by maintaining an adequate cerebral blood flow in case of blood pressure changes. Cannulation of great blood vessels and alterations of pulsatile flow patterns during ECMO (Extracorporeal membrane oxygenation) alters cerebral autoregulation. This project provides a reliable methodology that can assess the degree of cerebral autoregulation impairment of ECMO patients and examine if it can be correlated or predictive of neuroimaging abnormalities. Initially, we used the normal WTC MATLAB code to obtain a time-frequency map. Then we calculated the in-phase percent significance and used the resultant values to determine the Scale Averaged Percent Significance of Coherence (SASC) specifically in ranges 0-2.5-hour scale. The results showed that the lower the new SASC (as a Cerebral Autoregulation

index), the better the brain is. Comparing SASC to the MRI consensus, the average autoregulation index is >10% which is consistent with the ECMO outcome indicating mild neurological injury, meaning SASC can be predicative for ECMO patients. WTC during the total ECMO duration would show a clearer correlation with clinical outcome, thus further studies are needed to analyze that along with taking more patients into consideration (in addition to the current fourteen).

TABLE OF CONTENTS

Appendix

LIST OF ILLUSTRATIONS

LIST OF TABLES

CHAPTER 1

INTRODUCTION

1.1 Background

Cerebrovascular impairment can result in hemorrhagic and ischemic complications commonly seen in patients supported on ECMO. Extracorporeal membrane oxygenation (ECMO), also called a heart-lung machine, is a life-supporting therapy for critically ill patients with severe respiratory and/or cardiovascular failure (Tsuji et al., 2000). It was developed in the late 1960s by a team led by Robert H. Bartlett and first used successfully in 1971. It was a groundbreaking technology that quickly spread so much so that by 2009, ECMO was used worldwide in the treatment of severe lung failure (Modic, 2021). Despite the advancement and fame, ECMO is still posed with limitations such as inconsistent blood flow and pressure that call for urgent solutions. Studies showed an increased chance of stroke (part of the brain is damaged by loss of blood or by a blood vessel that bursts) mostly in ECMO survivors (Rossong et al., 2022). Further studies by Rossong et al. also provided evidence that cerebral autoregulation impairment during ECMO was related to the patients' neurological outcomes. A study on the long-term survival and quality of life after ECMO showed that 5-year survival is favorable for patients who endure the initial 30 days post cannulation, and survivors suffer from long term variable health related quality of life impairments (Rossong et al., 2022). Therefore, long term follow-up after discharge is required.

A better understanding of poor autoregulation-related physiological mechanisms is essential for developing new effective interventions to improve clinical outcomes. In addition, there is a lack of methodology that can quantify cerebral autoregulation non-invasively and reliably at the bedside. In the last decade, significant progress has been made in developing methods to assess cerebral autoregulation based on spontaneous oscillations in blood pressure, CBF, and cerebral oxygenation (Panerai, 1998).

Transfer function and other analysis methods for dynamic systems have been developed to assess cerebral autoregulation in the face of dynamic changes in blood pressure, referred to as dynamic cerebral autoregulation (Liu et al., 2015). These methods are often based on an assumption that changes in blood pressure and cerebral hemodynamics are stationary (i.e., do not change with time) while, in reality, the latter are non-stationary, particularly under pathophysiological conditions (Panerai, 2014). This highlights the need for better tools to characterize the non-stationary aspects of cerebral autoregulation hence the WTC method.

Wavelet transform coherence (WTC) is a time-frequency domain analysis that characterizes the cross correlation and relative phase between two signals without a priori assumptions of linearity and stationarity (Tian et al., 2016).

1.2 Significance and Objective of the Project

This research is critical in the advancement of the biomedical field, especially research, since it provides a reliable methodology that can determine the status of cerebral autoregulation during ECMO therapy. This would also serve as a biomarker that may predict early indications of neurological injury in pediatric ECMO patients which is paramount for optimization of bedside management to improve clinical outcomes. That

way the caretakers would perceive the degree of brain damage before it is too late. It would eventually help answer the questions: "does cannulation cause cerebral autoregulation impairment?" Or is the opposite true that "cerebral autoregulation impairment causes patients to have to undergo the ECMO therapy."

1.3 Summary of Peer-Reviewed Scholarship [Literature Review]

Continuous wavelet transform (CWT) is a powerful mathematical tool for time-frequency domain analysis of stationary and nonstationary time series (Torrence and Compo, 1998; Mallat, 1999). Wavelet coherence analysis, based on CWT, characterizes intermittent cross-correlations between two time series at multiple time scales (Grinsted et al., 2004), which makes no assumption about the stationarity of input signals. In their 2015 article on the matter, Liu et al. discussed how "the healthy brain is protected by cerebral autoregulation, which maintains an adequate cerebral blood flow (CBF) in face of blood pressure changes" (Tian et al., 2017). They continued by explaining that "cannulation of great blood vessels and alterations of pulsatile flow patterns during ECMO also play a role in altered cerebral autoregulation" (Tian et al., 2017). They demonstrated how they implemented WTC to assess the degree of cerebral autoregulation impairment in neonatal and pediatric ECMO and evaluated its usefulness as an early predictor of acute neurological complications. They did so by continuously monitoring cerebral autoregulation throughout the course of ECMO therapy. Surprisingly, they found intra-ECMO autoregulation impairment was apparent even before clinically observable changes occur at the bedside. Furthermore, the degrees of cerebral autoregulation impairment derived from WTC correlated with the patients' neuroimaging abnormalities (Tian et al., 2017). When neuroimaging was conducted during and/or after ECMO as a standard of care, the

abnormalities were evaluated based on a scoring system that had been previously validated among ECMO patients. The results showed that of the 25 patients that they had, 8 (32%) had normal neuroimaging, 7 (28%) had mild to moderate neuroimaging abnormalities, and the other 10 (40%) had severe neuroimaging abnormalities (Tian et al., 2017).

In addition, the degrees of cerebral autoregulation impairment quantified based on WTC showed significant correlations with the neuroimaging scores ($R=0.66$; $p < 0.0001$) where R^2 is the statistical significance between the two paired signals, which were the spontaneous MAP and SctO2 fluctuations in their study. Due to these results and based on their observation, evidence that cerebral autoregulation impairment during ECMO was related to the patients' neurological outcomes was provided.

This is confirmed by a 2016 study similarly conducted by Tian et al. still examining the wavelet coherence analysis. They stated that:

> We introduced wavelet coherence analysis (WCA) to assess dynamic cerebral autoregulation in newborns with hypoxic-ischemic encephalopathy (HIE). All hemodynamic data, including mean arterial pressure (MAP) and SctO2, were recorded continuously during the first 72 h of life under hypothermic therapy, then WCA was performed to quantify the spectral power and the dynamic relationship between spontaneous oscillations in MAP and SctO2. Wavelet-based metrics of phase, coherence and gain were derived for quantitative evaluation of cerebral autoregulation. (p.2 para.2, Tian et al., 2016).

Their results were comparing these metrics (i.e., wavelet-based metrics of phase, coherence, and gain) for clinical magnetic resonance imaging (MRI) and

neurodevelopmental outcomes to reveal short- and long-term neurologic complications in HIE patients.

In this project, I am building off of Tian et al.'s 2016 findings, still using their Montecarlo method. I will incorporate the pressure-passive state of cerebral autoregulation (i.e., the patient's changes in blood pressure cause simultaneous changes in cerebral oxygenation in the same directions). This is a vital sign of an impaired autoregulation system and results in significant in-phase coherence between the MAP and SctO2 signals (Soul et al., 2007). My contribution to this ongoing research is looking at the coherence between mean arterial pressure and cerebral oxygen saturation before and after cannulation and comparing it to the clinical outcomes. The hope is to devise a methodology that can be automated to generate prognostic values for improved bedside management of ECMO patients.

CHAPTER 2

METHODOLOGY

2.1 Subject and Data Preprocessing

The study was approved by the institutional review board at the University of Texas Southwestern Medical Center (UT-SW), Dallas, and informed consent was waived. The patients' spontaneous fluctuations of mean arterial pressure (MAP) and cerebral tissue oxygen saturation (SctO2) were continuously measured during the ECMO run and recorded in a patient list to indicate the patient ID, gender (for some), cannulation and decannulation date and time as shown in Table 2.1.

Table 2.1: Patient list collected by at the University of Texas Southwestern Medical Center, Dallas

Patient ID	Record ID	Age	M/F	Pre-ECMO (hours)	Cannulation Date	Cannulation time	Decannulation date	Decannulation time	ECMO duration (hours)	ECMO type	Neuro Imaging	Neuroimaging date
1			F		1/28/2021	17:05	2/28/2021	7:25			CTH	2/18/2021
2			F		6/3/2021	13:41	6/7/2021	12:35			MRI	6/24/2021
3			M		6/7/2021	6:20	6/10/2021	11:30			MRI	6/14/2021
4			M		7/17/2021	21:49	7/22/2021	14:20			CTH	7/29/2021
5			M		7/30/2021	8:30	8/4/2021	12:15			MRI	8/6/2021
6					2/1/2021	8:45	2/7/2021	12:07			CTH	2/5/2021
7					4/11/2021	11:22	4/15/2021	15:31			CTH	4/14/2021
8					*10/1/2020*	*13:42*	*10/4/2020*	*10:00*			*head ultrasound*	*10/1/20 - 10/7/20*
9					5/13/2021	10:15	5/16/2021	8:55			MRI	5/19/2021
10					5/20/2021	11:08	5/24/2021	11:13			MRI	6/11/2021
11					6/29/2021	23:30	7/3/2021	8:45			MRI	7/12/2021
12					7/1/2021	20:25	7/5/2021	9:30			MRI	8/4/2021
13					7/2/2021	10:00	7/16/2021	12:50			MRI	9/2/2021
14					*7/10/2021*	*14:14*	*7/12/2021*	*12:15*			*Ultrasound*	
15					*7/14/2021*	*8:47*	*7/17/2021*	*9:22*			*Ultrasound*	
16					8/6/2021	9:18	8/10/2021	7:31			CTH	8/15/2021
17					9/28/2021	12:50	10/9/2021	10:47			MRI	10/19/2021
18					10/9/2021	11:41	10/24/2021	11:45			MRI	10/26/2021
19					10/11/2021	21:34	10/15/2021	8:00			MRI	11/2/2021

Next, we obtained Excel data files of those patients from UT-SW in an .xls format as shown in Figure 2.1. To facilitate our analysis, we extracted columns A, I,J (i.e., the

time stamp, ARTm (mmHg) and rSO2-1 (%)) to create a new Excel file comprising of 6 columns only. The three other columns were manually input as seconds, minutes, hours, days, and automatically calculated using the formula bar; the frequency was kept as 1 in 5 seconds as shown in Figure 2.1.

timestamp	NBPs (mm	NBPd (mm	NBPm (mm	Model (n/	Temp (¿¿	etCO2 (mm	awRR (rpm	sMode (n/	RR (rpm)	SpO2 (%)	Perf (n/a)	Pulse (Spo	RhySta (n/	HR (bpm)	PVC (bpm	EctSta (n/	ARTm (mm	ARTs (mm	ARTd (mm	PPV (%)	rSO2-2 (%	rSO2-1 (%	BL-1 (%)	BL-2 (%)	AUC-1 (%)	AUC-2 (%)	PCTBL1 (%	PCTBL2 (%	TYPE (n/a	Temp_2 (¿	Tvesic (¿¿	Pulse (bpr
6/6/2021 18:07	158	99	117	Monitorin	35.3	27	26	MONITOR	26	79	0.56	134	Learning	ECG																	
6/6/2021 18:07					35.3	28	26	MONITOR	26	79	0.56	134	Learning	E	134																
6/6/2021 18:07					35.3	28	26	MONITOR	26	80	0.56	134	Learning	E	135																
6/6/2021 18:07					35.3	29	28	MONITOR	26	80	0.57	134	Learning	E	135	0															
6/6/2021 18:07					35.3	29	28	MONITOR	26	78	0.61	134	SV Rhythr		133	0															
6/6/2021 18:07					35.3	28	26	MONITOR	27	76	0.64	132	Sinus Rhy		122	1															
6/6/2021 18:07					35.3	28	27	MONITOR	26	75	0.65	132	Sinus Rhy		132	1															
6/6/2021 18:07					35.3	28	27	MONITOR	25	76	0.65	132	Sinus Rhy		133	1															
6/6/2021 18:07					35.3	28	27	MONITOR	26	77	0.65	133	Sinus Rhy		134	1															
6/6/2021 18:07					35.3	27	26	MONITOR	26	78	0.65	133	Sinus Rhy		134	1															
6/6/2021 18:07					35.3	28	26	MONITOR	27	78	0.65	132	Sinus Rhy		131	1															
6/6/2021 18:08					35.3	27	26	MONITOR	26	76	0.63	127	Sinus Rhy		126	1															
6/6/2021 18:08					35.3	27	26	MONITOR	26	76	0.63	124	Sinus Rhy		123	1															
6/6/2021 18:08					35.3	27	26	MONITOR	26	77	0.63	121	Sinus Rhy		120	1															
6/6/2021 18:08					35.3	27	26	MONITOR	26	76	0.63	119	Sinus Rhy		118	1															
6/6/2021 18:08					35.3	28	26	MONITOR	26	76	0.63	116	Sinus Rhy		116	1															
6/6/2021 18:08					35.3	27	26	MONITOR	26	77	0.63	119	Sinus Rhy		123	1															
6/6/2021 18:08					35.3	27	26	MONITOR	26	77	0.61	131	Sinus Rhy		133	0															
6/6/2021 18:08					35.3	27	26	MONITOR	26	77	0.56	135	Sinus Rhy		136	0															
6/6/2021 18:08					35.3	28	26	MONITOR	26	77	0.53	136	SV Rhythr		136	0															
6/6/2021 18:08					35.3	28	26	MONITOR	26	76	0.54	136	SV Rhythr		136	0															
6/6/2021 18:08	156	97	116		35.3	27	26	MONITOR	26	74	0.57	137	SV Rhythr		138	0															
6/6/2021 18:08					35.3	27	26	MONITOR	27	73	0.59	139	SV Rhythr		139	0															
6/6/2021 18:09					35.3	27	26	MONITOR	26	73	0.63	140	SV Rhythr		140	0															
6/6/2021 18:09					35.3	27	26	MONITOR	26	73	0.72	140	SV Rhythr		141	0															
6/6/2021 18:09					35.3	28	26	MONITOR	26	73	0.82	141	SV Rhythr		141	0															
6/6/2021 18:09					35.3	28	26	MONITOR	25	73	0.9	141	SV Rhythr		142	0															
6/6/2021 18:09					35.3	28	26	MONITOR	26	74	0.96	142	SV Rhythr		142	0															
6/6/2021 18:09					35.3	28	26	MONITOR	26	74	1.01	142	SV Rhythr		142	0															
6/6/2021 18:09					35.3	28	26	MONITOR	26	74	1.07	141	SV Rhythr		141	0															
6/6/2021 18:09					35.3	28	26	MONITOR	26	74	1.08	141	SV Rhythr		141	0															
6/6/2021 18:09					35.3	29	26	MONITOR	26	74	1.08	141	SV Rhythr		141	0															
6/6/2021 18:09					35.3	28	26	MONITOR	26	74	1.06	142	SV Rhythr		143	0															
6/6/2021 18:09					35.3	28	26	MONITOR	26	74	1.04	143	SV Rhythr		143	0															
6/6/2021 18:09					35.3	28	26	MONITOR	26	74	1	143	SV Rhythr		143	0															
6/6/2021 18:10					35.3	28	26	MONITOR	26	74	0.99	142	SV Rhythr		143	0															
6/6/2021 18:10					35.3	29	26	MONITOR	26	74	0.98	143	SV Rhythr		143	0															
6/6/2021 18:10					35.3	28	26	MONITOR	26	75	0.95	142	SV Rhythr		143	0															
6/6/2021 18:10					35.3	28	26	MONITOR	26	76	0.91	143	SV Rhythr		143	0															
6/6/2021 18:10					35.3	28	26	MONITOR	27	76	0.88	143	SV Rhythr		143	0															
6/6/2021 18:10					35.3	27	26	MONITOR	26	75	0.84	143	SV Rhythr		143	0															
6/6/2021 18:10					35.3	29	27	MONITOR	27	76	0.8	142	SV Rhythr		142	0															
6/6/2021 18:10					35.3	27	27	MONITOR	26	76	0.78	143	SV Rhythr		143	0															
6/6/2021 18:10					35.3	29	27	MONITOR	25	75	0.76	144	SV Rhythr		145	0															
6/6/2021 18:10					35.3	28	26	MONITOR	26	76	0.74	144	SV Rhythr		144	0															
6/6/2021 18:10					35.3	28	26	MONITOR	25	76	0.72	143	SV Rhythr		144	0															
6/6/2021 18:10					35.3	28	26	MONITOR	26	76	0.69	142	SV Rhythr		142	0															
6/6/2021 18:11					35.3	28	26	MONITOR	26	76	0.68	141	SV Rhythr		140	0															
6/6/2021 18:11					35.3	28	26	MONITOR	26	76	0.68	141	SV Rhythr		138	0															
6/6/2021 18:11					35.3	28	26	MONITOR	26	76	0.68	140	SV Rhythr		139	0															

Figure 2.1: Patient 3 Excel data file of the full ECMO run only showing 51 rows out of 221,074.

Some patients' files (except patients 1,2,3,5) that were sent as MATLAB files were directly converted to the 7 columns Excel file like the one shown in Table 2.2. We proceeded to sort through the columns to filter out the empty cells making sure that the beginning and end cells have values and are of the same length (hence why patient 3's columns were reduced from 221,074 as shown in Table 2.1 to 93,091 columns as shown in Table 2.2.

Table 2.2: Patient 3 downsized to 7 columns (after extracting columns A, I, J) from the full Excel file. Only 38/93091 are shown here.

timestamp	second	minutes	hours	days	ARTm	rSO2_1
6/7/2021 2:18	0	0	0	0	73	57
6/7/2021 2:18	5	0.083333	0.001389	0	75	58
6/7/2021 2:18	10	0.166667	0.002778	0	75	59
6/7/2021 2:18	15	0.25	0.004167	0	72	57
6/7/2021 2:18	20	0.333333	0.005556	0	69	57
6/7/2021 2:18	25	0.416667	0.006944	0	70	57
6/7/2021 2:18	30	0.5	0.008333	0	73	57
6/7/2021 2:18	35	0.583333	0.009722	0	74	58
6/7/2021 2:18	40	0.666667	0.011111	0	76	59
6/7/2021 2:18	45	0.75	0.0125	0	75	58
6/7/2021 2:18	50	0.833333	0.013889	0	72	57
6/7/2021 2:18	55	0.916667	0.015278	0	72	57
6/7/2021 2:19	60	1	0.016667	0	74	58
6/7/2021 2:19	65	1.083333	0.018056	0	76	58
6/7/2021 2:19	70	1.166667	0.019444	0	76	58
6/7/2021 2:19	75	1.25	0.020833	0	74	57
6/7/2021 2:19	80	1.333333	0.022222	0	73	57
6/7/2021 2:19	85	1.416667	0.023611	0	72	57
6/7/2021 2:19	90	1.5	0.025	0	73	57
6/7/2021 2:19	95	1.583333	0.026389	0	72	58
6/7/2021 2:19	100	1.666667	0.027778	0	71	57
6/7/2021 2:19	105	1.75	0.029167	0	71	57
6/7/2021 2:19	110	1.833333	0.030556	0	71	57
6/7/2021 2:19	115	1.916667	0.031944	0	76	57
6/7/2021 2:20	120	2	0.033333	0	82	57
6/7/2021 2:20	125	2.083333	0.034722	0	84	57
6/7/2021 2:20	130	2.166667	0.036111	0	85	58
6/7/2021 2:20	135	2.25	0.0375	0	84	58
6/7/2021 2:20	140	2.333333	0.038889	0	82	58
6/7/2021 2:20	145	2.416667	0.040278	0	87	59
6/7/2021 2:20	150	2.5	0.041667	0	95	60
6/7/2021 2:20	155	2.583333	0.043056	0	95	60
6/7/2021 2:20	160	2.666667	0.044444	0	88	59
6/7/2021 2:20	165	2.75	0.045833	0	85	58
6/7/2021 2:20	170	2.833333	0.047222	0	86	58
6/7/2021 2:20	175	2.916667	0.048611	0	88	58
6/7/2021 2:21	180	3	0.05	0	88	57

Afterwards, we loaded the files in MATLAB and first specified the filtering parameters by replacing any middle NAN values (empty cells) to zero and indicated the start and end arrays. Also, we specified the parameter requirements by setting the arterial mean blood pressure between 30-100 such that anything out of that range is replaced by the previous value. Then, we used the movmean (A,12) method which returns an array of local 12-point mean values, where each mean is calculated over a sliding window of length 12 across neighboring elements of A to reduce the noise. After that, the mean (A) was used to calculate the normal average of 12 data points to reduce the data length.

2.2 Wavelet Coherence Analysis

The Wavelet coherence analysis decomposes a time series in time-frequency domain by successively convolving the time series with the scaled and translated versions of a mother wavelet function (Mallat, 1999). In analogy to Fourier analysis, a wavelet power spectrum of x(n) can be defined as the wavelet transformation of its autocorrelation function. In this study, we used a MATLAB-based software package for wavelet coherence analysis between the spontaneous oscillations of MAP (mean arterial blood pressure) and SctO2 (cerebral oxygen saturation). This software package employs a Morlet wavelet as the mother wavelet, which provides a good trade-off between time and frequency localization (Grinsted et al., 2004).

The sampling frequency used was 1/60 HZ, and the dynamic relationship between the MAP and SctO2 fluctuations was assessed based on the wavelet transform coherence (WTC) code that was run, generating a time frequency map. The x-axis gives the time whereas the y-axis gives the frequency which has been converted to the logarithmic scale (in units of hours) by inversing it. The color bar of the scale represents coherence between

0-1 whereby higher coherence between SO2 and ARTm implies abnormal/worse blood autoregulation.

2.3 Developing SASC

Next, we took a 1-hour window width of time (out of the full-time interval of the time-frequency map) from the x-axis to calculate the in-phase percent significance. Then we used a moving window of 1hour across the whole x-axis time frame which gave us the in-phase percent significance value of each specific frequency in that particular window. After running the 1-hour moving window over the full-time interval, it yielded a set of frequencies with percent significance for every window. Thus, the percentage significance for 24 one hour-windows before cannulation (which was set as the reference point) and 24 one-hour windows after cannulation was quantified.

For each window, we had the percentage significance for each y-axis value as a long scale (in hours) column that was initially plotted in categories of 0-0.5 hours, 0.5-2.5 hours, 2.5-10 hours, and 0-10 hours. We decided to only focus on the 0-2.5 scale region as it was most representative of coherence in the region of interest. This range is also an area outside the cone of influence (COI) hence omits any edge effect (unwanted data). Therefore, we averaged the percentage significance values from 0-2.5-hour scale for each 1-hour window and plotted it. The graph was one for the scale averaged percent significance of coherence (SASC) versus the window graphs.

2.4 Data Analysis

Different moving window ranges were used to see if a faster run-time would affect the results in terms of SASC values obtained. In addition to the aforementioned 1-hour window, we tried the 4-hour, 6-hour, and 8-hour window. The larger hour-window was used for patients with longer ECMO run times such as patient 7 who had 1457 hours (~61 days), but the end results were all computed at a 1-hour window time for consistency.

The time dependent SASC was obtained for each patient 24 hours prior to cannulation (PRE) and 24 hours after cannulation (POST) in a step of 1 hour. The different patients were studied at a similar SASC and time scale (i.e., same-length x and y axes) to analyze any similar pattern before and after cannulation. Both the PRE and POST values were averaged separately to analyze the ratio of difference between them. Finally, a two-tail t-test was computed in Excel to analyze the significance of the difference observed.

Further analysis was done to compare the relationship between SASC and ARTm, ARTm and RSO2 and finally SASC and the MRI consensus (which is a general agreement or set of guidelines developed by experts in the field of magnetic resonance imaging (MRI)).

CHAPTER 3

RESULTS AND FINDINGS

Twenty-six children were under ECMO therapy for days to months for moderate and severe neuroimaging abnormalities during the study period. Exclusions were made according to the viability of the data collected for WTC analysis (e.g., cannulation time was indicated, availability of data before or after cannulation and ARTm and rSo2 recorded). Thus, fourteen children had complete monitoring data and were analyzed in this report. Individual characteristics and clinical outcomes of these neonates are summarized in the figure below.

Patient #	Cannulation Date	Cannulation Time	Full time	Cannulation Index	# of windows before cannulation (1hr)	# of windows after cannulation (1hr)	# of windows after cannulation (4hrs)
2	6/3/2021	1:41:00 PM (hr 4.94)	246 hrs	3563	4	24	59
3	6/7/2021	6:20:00 AM (hr 4.03)	129 hrs	2910	4	24	29
4	7/17/2021	9:49:00 PM (hr 19.19)	529 hrs	13823	19	24	127
5	7/30/2021	8:30:00 AM (hr 21.8)	244 hrs	15703	21	24	55
6	2/1/2021	8:45:00 AM (hr 12.94)	157 hrs	9319	12	24	36
9	5/13/2021	10:15:00 AM (hr 22.72)	126 hrs	16361	22	24	25
10	5/20/2021	11:08:00 AM (hr 40)	240 hrs	28967	40 (did 25 for AUC)	24	49
12	7/1/2021	8:25:00 PM (#hr 1.7)	984 hrs	1239	1	24	245
13	7/2/2021	10:00:00 AM (hr 142.81)	1317 hrs	102831	142 (did 24)	24	54
16	8/6/2021	9:18:00 AM (hr8.74)	229 hrs	6294	8	24	55
17	9/28/2021	12:50:00 PM (hr 99.56)	271 hrs	71674	99 (did 25 for AUC)	24	43
18	10/9/2021	11:41:00 AM (hr 62.09)	619 hrs	46872	65 (did 25 for AUC)	24	138
19	10/11/2021	9:34:00 PM (hr 290.5)	425 hrs	209173	291 (did 25 for AUC)	24	33
7	4/11/2021	11:22:00 AM (hr 1256)	1457 hrs	904376	1267 (did 25 for AUC)	24	47

Figure 3.1: Information table of all patients with viable data, and number of windows calculated for. AUC (mentioned in column 6) represents the “area under the curve” (which is the integrated/summed percent significance of coherence, calculated before averaging for SASC).

The dynamic relationship between the MAP and SctO2 fluctuations was assessed based on the wavelet transform coherence (WTC) code that was run, generating a time frequency map.

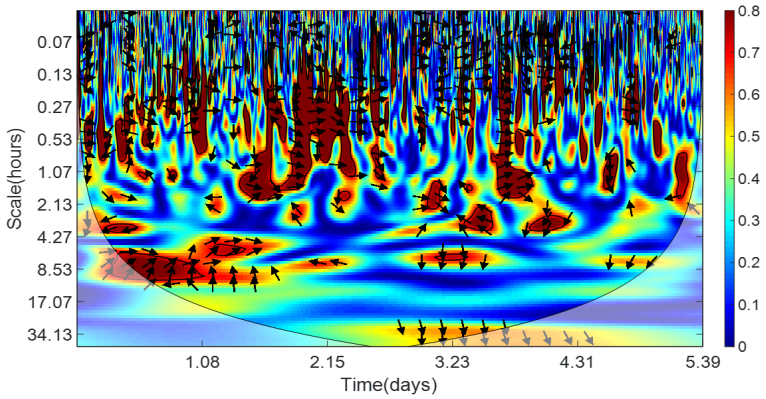

Figure 3.2: Time-Frequency map whereby the x-axis represents time (in days), and the y-axis represents scale (which has been converted to the equivalent Fourier period). The black line contours designate areas of significant coherence, and the arrows designate the relative phase between MAP and SctO2 (a rightward pointing arrow indicates in-phase coherence between the two signals). The color bar of the scale represents coherence between 0-1 whereby higher coherence between SO2 and ARTm implies abnormal/worse blood autoregulation.

To better see and analyze the trend of coherence before and after cannulation, we plotted an all-patients graph showing their cannulation at the same time. This was done by subtracting each one's cannulation hour from the total hours recorded to make cannulation fall at hour zero so everything before it is negative while all after is positive.

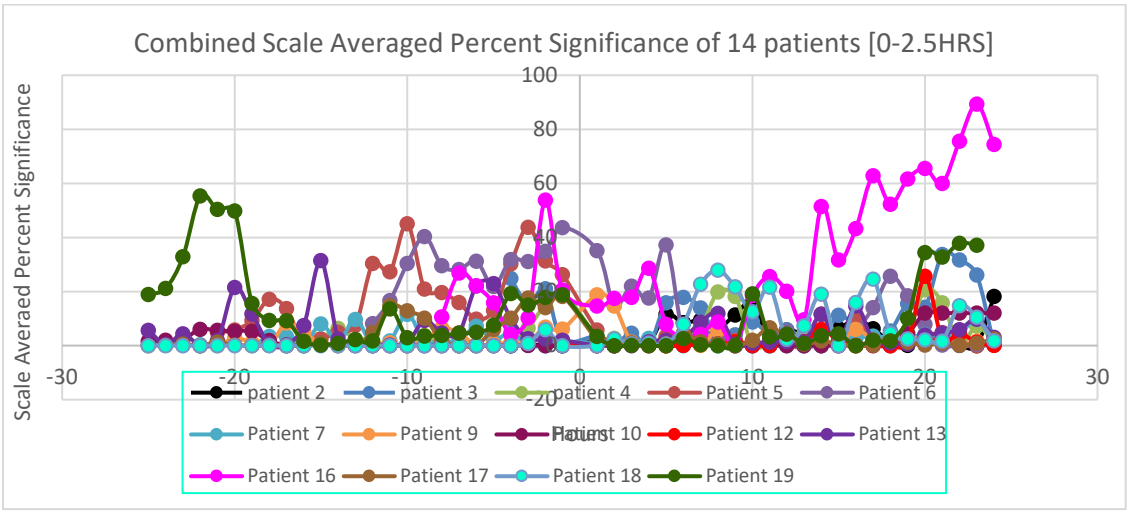

Figure 3.3: Combined scale averaged percent significance of coherence of 14 patients just looking at the range of 0-2.5 hrs.

Furthermore, still trying to analyze and spot a commonly re-occurring trend, we put two by two patients per page and ensured they were of the same y-axis scale and marked their cannulation points with a red line on all graphs for comparison purposes. Figures 4 and 5 below show the results. Although it was not the case for all, a clear trend to notice is the downward dip of the SASC curves right after cannulation but it would spring up again in the following hours.

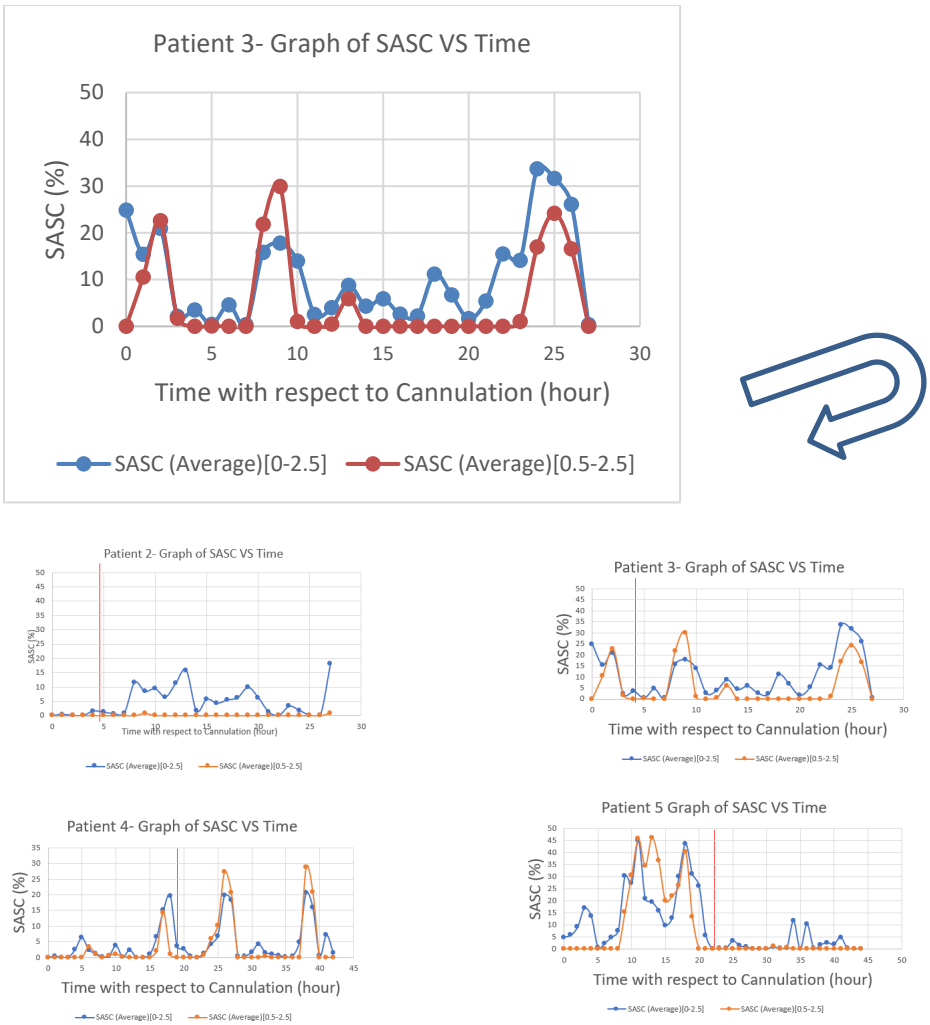

Figure 3.4: An individual graph of patient 3's SASC vs time comparison; a comparison graphs of patients 2,3 and 4,5 looking at their SASC vs time graph to analyze any common pattern before/after cannulation.

Furthermore, we plotted the arterial mean blood pressure (ARTm) against that SASC graphs for all patients individually as well as their ARTm versus rSo2 (oxygen saturation). This was done in a bid to analyze and compare their patterns while looking for any similarities. For better comparison, the characteristic variables were plotted on the same x-axis scale and double y-axis (of hours/days) with ARTm being the secondary axis.

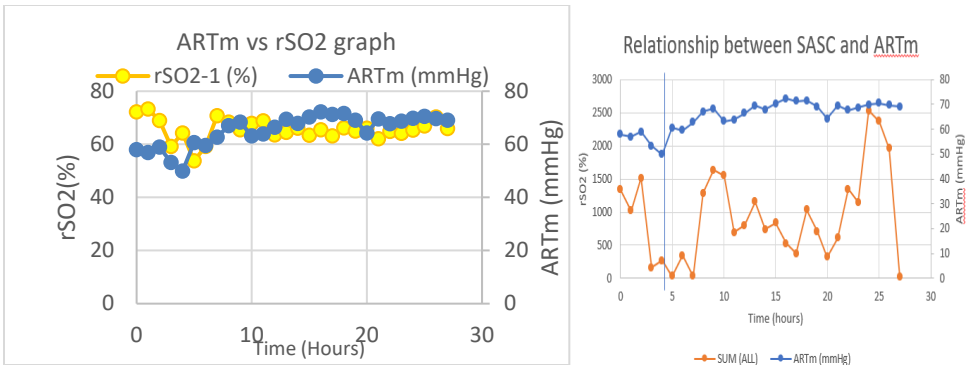

Figure 3.5: Comparison graph of ARTm vs Rso2 and SASC vs ARTm for patient 3

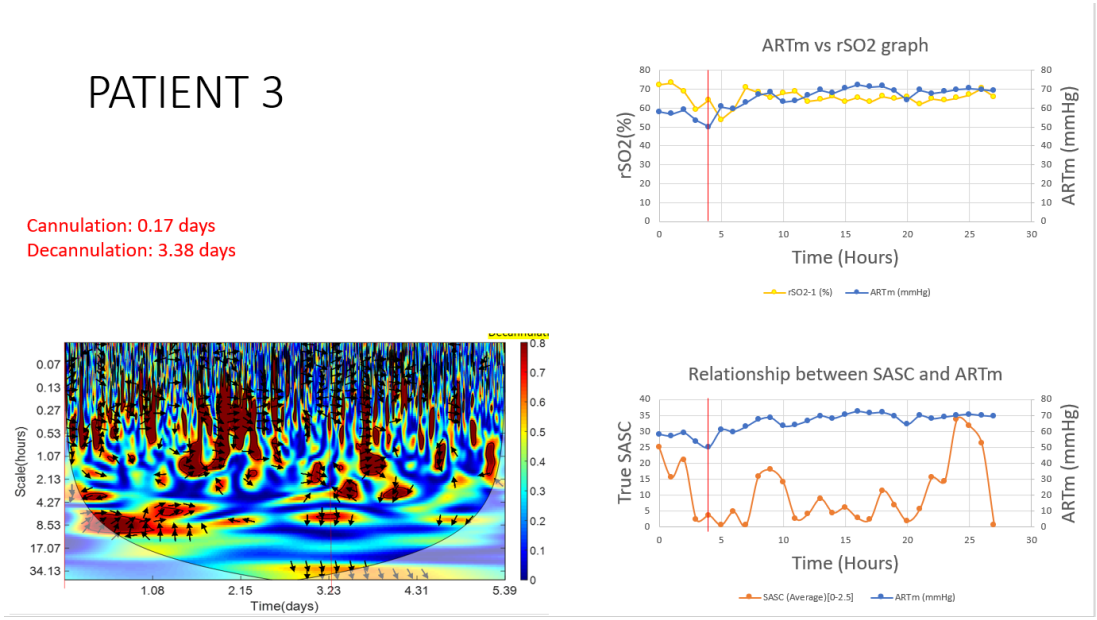

Figure 3.6: Comparing the variables to the time-frequency map to analyze the causes of sudden and extreme peaks and troughs.

The time dependent SASC was obtained for each patient 24 hours prior to cannulation (PRE) and 24 hours after cannulation (POST) in a step of 1 hour. Both the PRE and POST values were averaged separately to analyze the ratio of difference between them. A two-tail t-test was computed in Excel to analyze the significance of the difference observed.

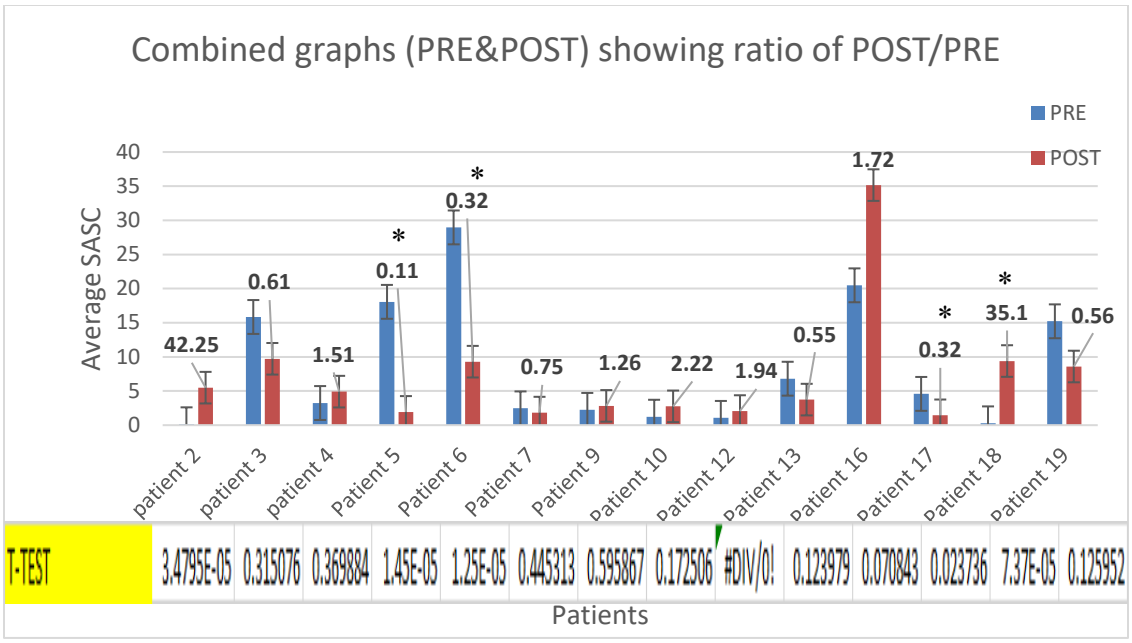

Figure 3.7: Combined bar plots of all 14 patients' PRE and POST cannulation SASC averages over 24 hours showing their ratio differences as well as the t-test results. * Indicates averages of significant difference. Patients 12 had an error since it only had one value pre-cannulation.

Finally, still in the comparative section, all patients SASC averages 24 hours prior to cannulation and the same post cannulation were averaged and compared to the clinical MRI consensus. The trendlines and R-values of the respective graphs were also computed for better analysis hence conclusion drawing.

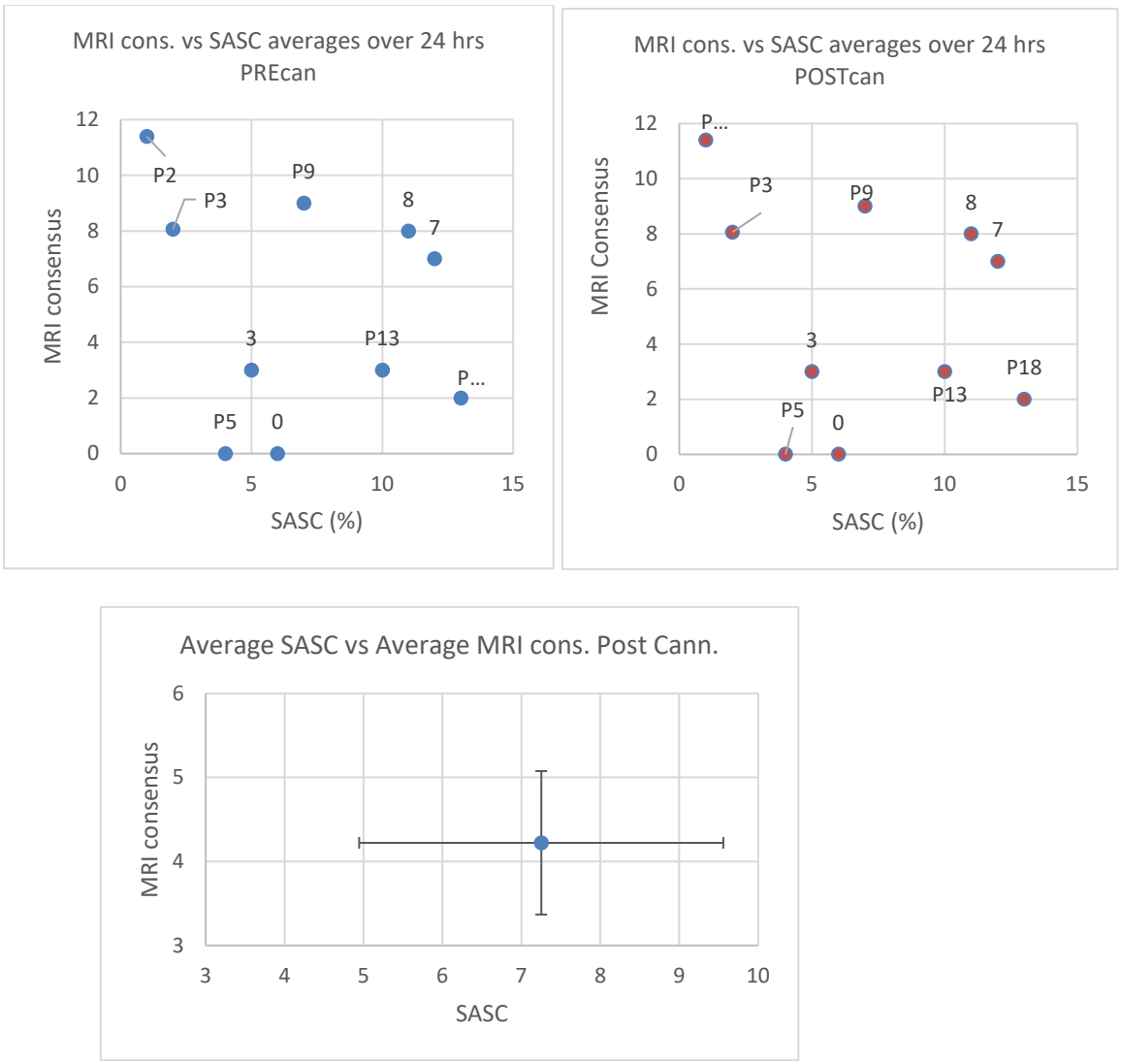

Figure 3.8: MRI consensus vs SASC averages over 24 hours during Pre and Post cannulation. (Central bottom) single point plot of the average SASC vs average MRI consensus post cannulation with SEM (standard error of mean) bars.

Finally, different moving window ranges were used to see if a faster run-time would affect the results in terms of SASC values obtained. In addition to the previously mentioned 1-hour window, we also tried the 4-hour, 6-hour, and 8-hour window.

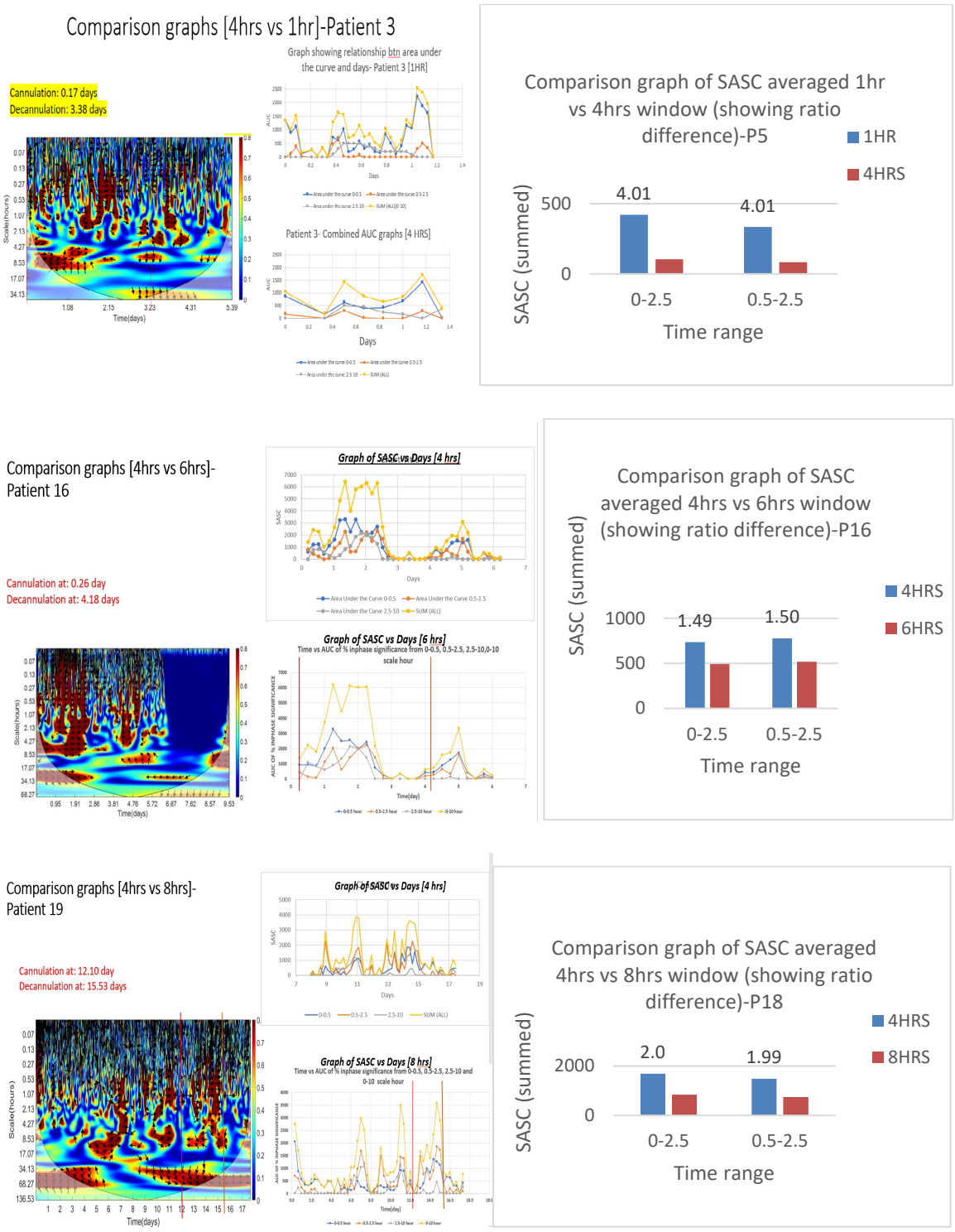

Figure 3.9: Comparative graph of SASC averaged at different window lengths (showing ratio differences). (Top) 1-hour vs 4-hour window. (MIDDLE) 4hour vs 6hour window. (BOTTOM) 4hour vs 8-hour window.

CHAPTER 4

DISCUSSION

The current study assessed cerebral autoregulation in pediatric patients during ECMO therapy by using a novel wavelet coherence analysis to characterize the dynamic relationship between the spontaneous mean arterial blood pressure (MAP) and cerebral oxygen saturation (SctO2) oscillations, considering 24 hours before cannulation and 24 hours after. The wavelet-derived metrics of phase and coherence for quantitative evaluation of cerebral autoregulation indicate a potential to use this methodology to predict clinical outcomes during early phase of neonatal care at the bedside (Tian et al., 2016).

In a similar research study evaluating the dynamic cerebral autoregulation in neonatal hypoxic–ischemic encephalopathy, Tian et al. explained how using SctO2 as an index of cerebral blood flow dynamics gives more accurate data as it is less sensitive to movement artifact and therefore more suitable for the purpose of long-time scale recording (Tian et al., 2016). They also added that SctO2 has been validated to correlate well with MRI arterial spin label cerebral blood flow in the setting of encephalopathy (Wintermark et al., 2014). The significant, intermittent in-phase coherence between the MAP and SctO2 changes indicated that the patient's cerebral oxygenation was passive to the blood pressure changes during hypothermia, a vital sign of an impaired autoregulation system (Tian et al., 2016). This supports the results obtained above that showed autoregulation disruption noticed a stronger coherence between the ARTm and Rso2.

All patients showed an oscillating trend of the scale averaged percent significance of coherence with time, and when put together to compare the pre-cannulation and post cannulation trends, the t-test showed that 31% of them (i.e., 4 out of 13) had a significant difference. Their relative average changes between the PRE and POST values of all patients further support this conclusion as we see that half of them had a higher pre-cannulation average while the remaining half had a higher post cannulation average. This non-stationarity of the input signals over multiple time scales is evidence of autoregulation. This was confirmed in a past study by Latka et al. (2005) demonstrating that the phase dynamics between the spontaneous changes in MAP and CBF velocity measured in the middle cerebral artery (MCA), which was based on wavelet analysis, accounted for most of the nonlinear and non-stationary properties of cerebral autoregulation. Thus, assessment of dynamic cerebral autoregulation using wavelet coherence makes no assumption about the stationarity of input signals (Tian et al., 2016).

Moreover, our findings give a clear indication that time-dependent coherence calculations are insensitive to the selection of window length. Here we started off by using a window length of 4 hours but reverted to using 1-hour to accommodate patients that had very little data pre-cannulation e.g., patient 12 whose data only had one hour PRE. We also tried using an 8-hour window length to quicken the computation time for patients whose data goes on for about a month. In the end, the comparison between graphs at 1-h, 4-h, 6-h, and 8-h window lengths gave relatively similar results with the only difference being the amount of datapoints generated. The summation of the 4-h data per patient yielded four times that of 1-h window length of the same patient while their data averages appeared to be the same. This was also the case for the 6-h and 8-h comparisons. These results can be

explained by the fact that cerebral autoregulation is a time-scale dependent phenomenon. In their 2016 study on the matter, Tian et al.'s main findings indicated that Significant in-phase coherence between the MAP and SctO2 oscillations occurred mostly in shorter time scales of ≤80 min with a peak of around 7.5 min. Thus, our finding of the in-phase coherence between MAP and SctO2 is in line with the previous findings of a pressure-passive status of impaired cerebral autoregulation that corresponded to changes occurring over several minutes that is more apparent when run at a smaller window length to account for every minute rather than a larger window length that shows the overall pattern. This finding can be used for further engineering advancements to automate our methodology to a faster computation time that yields real-time SASC values for bedside clinical improvements.

Finally, Wavelet-based metrics of phase, coherence and gain were derived to quantify the severity of impaired cerebral autoregulation (Tian et al., 2017). We saw that the lower the new SASC (as a Cerebral Autoregulation index), the better the brain is. Comparing SASC to the MRI consensus, the average autoregulation index is less than 10% which is consistent with the ECMO outcome indicating mild neuro-injury meaning that the autoregulation is disrupted a bit but not severely. This is the case for all patients except patient 4 because all are below an MRI consensus of 10. A score of 10 or above is for severe neurological injury for ECMO. For Tian et al.'s 2017 study their preliminary findings suggest that these measures appear to be useful for predicting the short-term and long-term clinical outcomes following hypothermic therapy. It is safe to assume the same for this study too, especially since the single-point averaging graph of SASC vs MRI consensus comes to a point that approximately close considering the current sample size

of n=14. That point is at 7.5,4.2 for SASC vs MRI consensus respectively thus confirming the predicted trend that poor autoregulation indicates a higher SASC value and a lower MRI consensus value (relating to worse clinical outcomes).

However, this study has several limitations. First, the current data was collected from a small sample of patients (n = 14), which limited the ability to address moderate and severe neurological injury separately. The findings in the study need to be replicated in larger groups of patients. More patients' data will help confirm the hypothesis for the prediction of ECMO patients, and would help stabilize the mean, take out the outliers and draw a better conclusion between SASC and MRI. Secondly, WTC during the 24-hour cannulation showed good correlation with clinical outcome or MRI consensus but running it for the total ECMO duration might surely be a better predictor. Since MRI is a cumulative injury indicator, most damage is expected to happen during 24 hours but that is not necessarily always the case.

CHAPTER 5

CONCLUSION

Wavelet coherence analysis is a suitable and powerful tool to characterize and quantify the dynamic status of cerebral autoregulation during a long-lasting treatment such as the ECMO therapy. Based on this method, significant in-phase coherence between spontaneous oscillations in MAP and SctO2 were found in the pediatric patients during the therapy, and it appeared to be related to worse clinical outcomes. These findings support the feasibility of using this method to assess cerebral autoregulation impairment in ECMO patients as well as its potential predictive values for short- and long-term clinical measures in these patients.

APPENDIX A

CONVERTING A .MAT FILE TO .CSV

```
clear all;  clc; close all;
% load('Patient12_t3_data.mat');
load('C:\Users\research\Desktop\Sylvine\UTSW_ECMO_Data\UTSW_ECMO_Data\Pati
ent18_t3_data.mat')

% to find out nan value and convert it to zero
for i=1:size(ARTm_mmHg,2)
   if isnan(ARTm_mmHg(i))
      ARTm_mmHg(i)=0;
   end
end
for i=1:size(rSO2_1_percent_,2)
   if isnan(rSO2_1_percent_(i))
      rSO2_1_percent_(i)=0;
   end
end

%csvwrite('Patient7_t3_data.mat',timestamp);

for ii= 1:length (timestamp)
   timestamp2 (ii,:)= convertCharsToStrings(timestamp(ii,:));
end
z=[rSO2_1_percent_',ARTm_mmHg'];
```

APPENDIX B

FILTERING THE DATA, SPECIFYING THE READING PARAMETERS

```
for i=1:size(a.data,1) % from first to size of a.data first row
   for k=5:6
      if isnan(a.data(i,k))
      a.data(i,k)=0
      end
   end
end
clear i k

first_day = find(a.data(:,3)<=1457); % 24 hrs - 1, 48 hrs - 2, so on and so fort
first_strt = first_day(1,:); %first row of first_day
first_end = first_day(end,:);
cannulation_point=976469;

so2 = a.data(first_strt:first_end,5);
artm = a.data(first_strt:first_end,6);
% time= a.data(first_strt:first_end,3);

% k=1;
% count=0;
if artm(1,1)>=30 && artm(1,1)<=100
   for i=1:size(artm,1)
     if artm(i,1)>100 || artm(i,1)<30
        %dataset(k,1)= ARTm(i,1);
        artm(i,1)=artm(i-1,1);
%          count=count+1;
%          k=k+1;
     end
   end
else
   fprintf("The first number is below 30 or above 100")
end
%clear first_end first_strt i
clear i

% for moving average
window=12;% for 1 min window take window 12 as each data point is of 5 secs and 12
datapoints makes a window of 1 min
so2_avg=(movmean(so2,window));
artm_avg=(movmean(artm,window));
% time_avg=(movmean(time,window));

% so2_avg1=so2_avg(60:60:end);%taking average of every 60 points
% artm_avg1=artm_avg(60:60:end);
i=1;
```

```
j=12;
k=1;
while(i<=first_end)
   so2_avg1(k)=mean(so2_avg(i:j));
   artm_avg1(k)=mean(artm_avg(i:j));
%    time1(k)=mean(time_avg(i:j));
%z=[artm_avg1' so2_avg1'];
   i=i+12;
   j=j+12;
   k=k+1;
end
```

APPENDIX C

RSO2 AND ARTM CONVERSION AND AVERAGING CODE

```
%before cannulation
start_of_cannulation=floor(cannulation_point/12);
%cann_time_in_hour=cannulation_point/(12*60*24);
x=1;% window length i.e., 6 hours
fix=x*60;
no_loop=floor(start_of_cannulation/fix);
cons=floor(start_of_cannulation-(no_loop*fix));
if no_loop>24
   no_loop=24;
end

for k=1:no_loop
   So2_before(k)=mean(so2_avg(cons:cons+fix));
   ARTm_before(k)=mean(artm_avg(cons:cons+fix));
   cons=cons+fix;
end
So2_before=So2_before';
ARTm_before=ARTm_before';
%% after cannulation
end_of_cannulation=floor(cannulation_point/(12));
x=1;% window length i.e., 6 hours
fix=x*60;
cons=end_of_cannulation;
for f=1:24
   So2_after(f)=mean(so2_avg(cons:cons+fix));
   ARTm_after(f)=mean(artm_avg(cons:cons+fix));
   cons=cons+fix;
end
So2_after=So2_after';
ARTm_after=ARTm_after';
% So2_final=[So2_before So2_after];
% ARTm_final=[ARTm_before ARTm_after];
```

APPENDIX D

WAVELET TRANSFORM COHERENCE (WTC) MATLAB CODE

```
clear artm i j k so2 window first_strt
so2_avg1=so2_avg1';
artm_avg1=artm_avg1';
fs = 1/60; %new sampling rate = 1 sample every 300sec (5min)
[Rsq period sca coi sig95 aWxy freq] = wtc_any_fs(so2_avg1,artm_avg1,fs);

figure; set(gcf,'Position',get(0,'ScreenSize')); % to plot the figure in fullsize.
wtc_any_fs(so2_avg1,artm_avg1,fs);
colorbar;  set(gca,'Clim',[0
0.8],'fontsize',30);colormap('jet');xlabel("Time(days)"),ylabel("Scale(hours)");

% CONVERTING FREQUENCY IN Y SCALE TO HOUR SCALE
m=yticklabels;
m=str2num(m);
m=1./m % converting to time domain in sec
m=m./3600;
m = round(m,2);
yticklabels(m);

hour=first_end/(12*60);
day=hour/24;
diff=day/10;
hrs=([0:diff:day]);
xticks([0:diff*3600*24:day*24*3600]);% for day

xticklabels(round(hrs,2));
clear artm m hrs diff fs
```

APPENDIX E

SIGNIFICANCE CALCULATION

```
%IN HOURS.....................
clear sig951 freq1 period1 coi1 cone1 sig95_0_NIRS_c_NIRS_a_pre1 aWxy1 i
sig95_180_NIRS_c_NIRS_a_pre1 pha_0 pha_180 pha_270 pha_90
cann_time_in_hour=cannulation_point/(12*60);

new_cann_point=round((length(sig95)/hour)*cann_time_in_hour);
new_window_4_hours=round(length(sig95)/(hour))*1;
fix=new_window_4_hours;
freq1=freq';
cons=new_cann_point-fix;
%clear new_cann_point new_window_4_hours cann_time_in_day cannulation_point

% loop to run significance percentage for 1 pre cannulation window and 2 post
cannulation windows
for x=1:25
   sig951=sig95(:,cons:cons+fix);%(1440/24)*6=360 1440 has total time period of 24
hours, we only need 6 hours
   sig951(find(sig951< 1)) = 0;
   sig951(find(sig951>=1)) = 1;
   aWxy1=aWxy(:,cons:cons+fix);
   coi1=coi(cons:cons+fix);
   period1=period;
   % dividing into 4 quadrants
   pha_0 = ones(size(aWxy1));            pha_0(find(abs(aWxy1)>pi/4)) = 0;
   % pha_90 = zeros(size(aWxy));          pha_90(find((aWxy)>=pi/4 &
(aWxy)<=(3*pi/4) )) = 1;
   pha_180 = ones(size(aWxy1));          pha_180(find(abs(aWxy1)<pi*3/4)) = 0;
   % pha_270 = zeros(size(aWxy));         pha_270(find((aWxy)>=-3*pi/4 &
(aWxy)<=-(pi/4) )) = 1;

   cone1 = ones(size(sig951));
   for i = 1:length(coi1)
      cone1(find(period1>coi1(i)),i) = nan;
   end
   % percentage of sig95
   temp = nanmean(sig951.*pha_0.*cone1,2)./nanmean(cone1,2)*100;
   sig95_0_NIRS_c_NIRS_a_pre1 = temp;    % wavelet scale <240 mins
   sub_total(:,:,x)=sig95_0_NIRS_c_NIRS_a_pre1;
   % temp = nanmean(sig951.*pha_180.*cone1,2)./nanmean(cone1,2)*100;
   % sig95_180_NIRS_c_NIRS_a_pre1 = temp;  % wavelet scale <240 mins
   cons=cons+fix;
   disp(cons);
end

pre_sig=sub_total(:,:,1);
pre_sig1=sub_total(:,:,2);
```

```
pre_sig2=sub_total(:,:,3);
pre_sig3=sub_total(:,:,4);
pre_sig4=sub_total(:,:,5);
pre_sig5=sub_total(:,:,6);
post_sig1=sub_total(:,:,7);
post_sig2=sub_total(:,:,8);
post_sig5=sub_total(:,:,9);
post_sig6=sub_total(:,:,10);
```

REFERENCES

Grinsted, A., Moore, J. C., and Jevrejeva, S.: Application of the cross wavelet transform and wavelet coherence to geophysical time series, *Nonlin. Processes Geophys., 11*, 561–566, https://doi.org/10.5194/npg-11-561-2004, 2004.

Latka, M., Turalska, M., Glaubic-Latka, M., Kolodziej, W., Latka, D., West, B.J., 2005. Phase dynamics in cerebral autoregulation. Am. J. Physiol. Heart Circ. Physiol. 289, H2272–H2279.

Liu, X., Czosnyka, M., Donnelly, J., Budohoski, K.P., Varsos, G.V., Nasr, N., Brady, K.M., Reinhard, M., Hutchinson, P.J., Smielewski, P., 2015. Comparison of frequency and time domain methods of assessment of cerebral autoregulation in traumatic brain injury. J. Cereb. Blood Flow Metab. 35, 248–256

Modic, E. E. (2021, July 30). Advancing Artificial Lung Technology – ECMO. Today's Medical Developments. Retrieved November 10, 2022, from https://www.todaysmedicaldevelopments.com/article/artificial-lung-technology-ecmo-extracorporeal-membrane-oxygenation/

Panerai, R.B., 1998. Assessment of cerebral pressure autoregulation in humans—a review of measurement methods. Physiol. Meas. 19, 305–338

Panerai, R.B., 2014. Nonstationarity of dynamic cerebral autoregulation. Med. Eng. Phys. 36, 576–584

Rossong, H., Debreuil, S., Yan, W., Hiebert, B. M., Singal, R. K., Arora, R. C., & Yamashita, M. H. (2022). Long-term survival and quality of life after extracorporeal membrane oxygenation. *The Journal of thoracic and cardiovascular surgery*, S0022-5223(22)00204-5. Advance online publication. https://doi.org/10.1016/j.jtcvs.2021.10.077

Soul, J. S., Hammer, P. E., Tsuji, M., Saul, J. P., Bassan, H., Limperopoulos, C., Disalvo, D. N., Moore, M., Akins, P., Ringer, S., Volpe, J. J., Trachtenberg, F., & du Plessis, A. J. (2007). Fluctuating pressure-passivity is common in the cerebral circulation of sick premature infants. *Pediatric research*, *61*(4), 467–473. https://doi.org/10.1203/pdr.0b013e31803237f6

Tsuji, M., Saul, J. P., du Plessis, A., Eichenwald, E., Sobh, J., Crocker, R., & Volpe, J. J. (2000). Cerebral intravascular oxygenation correlates with mean arterial pressure in critically ill premature infants. *Pediatrics*, *106*(4), 625–632. https://doi.org/10.1542/peds.106.4.625

Tian, F., Morriss, M. C., Chalak, L., Venkataraman, R., Ahn, C., Liu, H., & Raman, L. (2017). Impairment of cerebral autoregulation in pediatric extracorporeal membrane oxygenation associated with neuroimaging abnormalities. *Neurophotonics*, *4*(4), 041410.

Tian, F., Tarumi, T., Liu, H., Zhang, R., & Chalak, L. (2016). Wavelet coherence analysis of dynamic cerebral autoregulation in neonatal hypoxic–ischemic encephalopathy. *NeuroImage: Clinical*, *11*, 124-132.

Torrence, C., & Compo, G. P. (1998). A Practical Guide to Wavelet Analysis, *Bulletin of the American Meteorological Society*, *79*(1), 61-78. doi: https://doi.org/10.1175/1520-0477(1998)079<0061:APGTWA>2.0.CO;2

BIOGRAPHICAL INFORMATION

Sylvine is working towards her Honors Bachelor degree in Biomedical Engineering. She is also actively involved in research with faculty and focuses on the medical imaging engineering discipline. She has previously worked on various other projects in the BME field such as Redesigning CPAP prongs for NICU babies, Meniscus Replacement Scaffold, Effects on Concentration and Brain Activity during Studying with Music, and the BIOCO Project that provides biogas from cow dung in Rwanda.

To broaden her perspective, she has also taken a minor in sustainable engineering. She aspires to gain the required experience and knowledge in addition to her skills and curiosity to contribute towards innovative approaches in research. In addition to being a factor in the development of advanced medical devices in necessitous communities, especially those in the great lakes' region of Africa, her homeland.